Available online at www.sciencedirect.com

ScienceDirect

Journal of the European Ceramic Society 29 (2009) 39–46

www.elsevier.com/locate/jeurceramsoc

The effect of BaO and Al_2O_3 addition on the crystallization behaviour of cordierite glass ceramics in the presence of V_2O_5 nucleant

V.K. Marghussian*, U. Balazadegan, B. Eftekhari-yekta

Ceramics Division, Department of Materials, Iran University of Science and Technology, Narmak, Tehran, Iran

Received 11 March 2008; received in revised form 24 May 2008; accepted 30 May 2008
Available online 10 July 2008

Abstract

The effect of V_2O_5 nucleant on crystallization of stoichiometric cordierite glass ceramics in the presence of various amounts of BaO and Al_2O_3 additives were investigated by DTA, XRD and SEM. It was shown that 3 wt.% V_2O_5 and 1.5 wt.% BaO were the optimum amounts of the additives effective in inducing both surface and bulk crystallization in the above glass ceramics.

This resulted in ~90 wt.% cordierite after a 3 h heat treatment at 1020 °C. The specimens possessing 4–5 wt.% Al_2O_3 in excess of the stoichiometric cordierite composition, developed mullite along with cordierite in the temperature range of 1045–1055 °C, whereas in the specimen containing 6 wt.% excess Al_2O_3, mullite was detected as the sole crystallization product.

Keywords: B. Microstructure-final; B. Electron microscopy; D. Glass ceramics; B. Mullite; Cordierite

1. Introduction

The outstanding thermo-mechanical, chemical and electrical properties of cordierite-based glass ceramic materials render them suitable for a number of applications ranging from radomes to integrated circuit substrates and from cookware to industrial heat exchangers. These materials are usually processed by heat treating glass articles of suitable composition with the aim of converting them to glass ceramic materials with cordierite as their major crystalline phase.

Many aspects of the process including the effect of composition, nucleating agents and heat treatment procedure upon the mechanical, thermal and electrical properties as well as the crystallization mechanisms and kinetics of these materials have been investigated and intensively discussed in literature.[1–15]

Mullite-based glass ceramics, on the other hand have attracted some attention in recent years owing to their interesting thermo-mechanical, chemical and optical properties. Several applications have developed for these glass ceramics such as dental materials, ceramic matrix composites and glazes for floor tiles.[16–18]

Cordierite–mullite materials fabricated via conventional ceramic route have been in use for many years for their good thermo-mechanical properties in some applications e.g., kiln furniture, but cordierite–mullite glass ceramics have attracted little attention.

The present study is concerned with the effect of BaO and Al_2O_3 additives on crystallization behaviour of glass specimens of stiochiometric cordierite composition. It was supposed that while BaO could act as a flux, lowering the relatively high melting temperature of cordierite glass, its addition because of the large size of cation could have relatively little detrimental effect on dielectric properties of the resulting glass ceramic material.

On the other hand it was proposed that the raising of Al_2O_3 content at the expense of MgO would result in crystallization of mullite along with cordierite, producing a mullite–cordierite glass ceramic.

In this work it was also decided to use V_2O_5 as a nucleating agent in this system. Very little reports have appeared in literature concerning the effectiveness of V_2O_5 as a nucleant in the devitrification of cordierite glass ceramics.

Devekey and Majumdar[19] evaluated V_2O_5 as an oxide of no sufficient ability to cause effective bulk nucleation in this system.

One of the present authors also observed and reported[20] the relative effectiveness of V_2O_5 in the crystallization of cordierite

---

* Corresponding author. Tel.: +98 21 73912814; fax: +98 21 77240480.
E-mail address: v_k_marghus@yahoo.com (V.K. Marghussian).

0955-2219/$ – see front matter © 2008 Elsevier Ltd. All rights reserved.
doi:10.1016/j.jeurceramsoc.2008.05.026

glass ceramics but the subject has never been explored in depth since then.

2. Experimental

2.1. Glass preparation

Table 1 gives the chemical compositions of various glasses studied. The composition C belongs to the stoichiometric cordierite with 10 wt.% TiO_2 addition and was solely used as a basis for comparison. The specimen V_1 was prepared by adding 3 wt.% V_2O_5 to the stoichiometric cordierite composition and compositions V_2, V_3 and V_4 were made by addition of 1.5, 5 and 10 wt.% BaO to specimen V_1, respectively.

Specimens M_1–M_4 were made by increasing the Al_2O_3 content of specimen V_2 at the expense of MgO in 2 wt.% (M1–M2) and 1 wt.% steps (M3–M4), respectively.

The raw materials used were reagent grade $BaCO_3$, MgO, Al_2O_3, TiO_2 and V_2O_5 powders. The source of SiO_2 was pure silica sand for making optical glass.

The glasses were melted in alumina crucibles at 1600–1650 °C range in an electric furnace for 2 h and were cast onto preheated stainless steel moulds. The glass specimens then were annealed at 600 °C for 1 h and furnace cooled.

2.2. Differential thermal analysis (DTA)

Differential thermal analysis were performed on the glass samples at the range 20–1200 °C using samples of <65 μm and 0.5–0.6 mm particles sizes (Shimadzu DTG 60 AH). Alumina was used as an inert reference material and the heating rate was 10 °C min^{-1}. Three specimens were used for each measurement.

2.3. X-ray diffraction (XRD) studies

In order to identify the crystallization products and determine their quantities the heat-treated samples were subjected to XRD analysis (Jeol JDX-8030 and Siemens-D500). In the course of heat treatment first a constant heating rate of 12 °C min^{-1} was adopted up to the dilatometric softening point ∼800 °C after which the rate was reduced to 2 °C min^{-1} and kept constant to the end of experiment. All samples were held at the first exothermic peak (if it existed) for 1 h and the second exothermic peak temperature for 3 h and then air cooled.

Cu K_α radiation was used in XRD examinations. Working voltage and current were 40 kV and 80 mA, respectively, and the step size and time were 0.04° and 0.75 s.

2.4. Microstructural examinations

The samples after polishing and etching in 5% HF solution were coated with a thin film of gold and subjected to SEM examinations (scanning electron microscope, Philips-XL 30 and Cambridge-S 360). The working voltage was 20 kV.

3. Result and discussion

3.1. DTA results

Fig. 1 depicts typical DTA traces and Table 2 summarizes the DTA results for some specimens. While specimen C exhibited two exothermic peaks, specimens V_1–V_4 and M_1–M_4 showed single exothermal effects. The first and second exothermic peaks, in the case of specimen C, can be attributed to the crystallization of μ-cordierite (β-quartz solid solution) and α-cordierite, respectively, and the single exothermic effects can be assigned to the crystallization of cordierite in specimen M_1, mullite + cordierite in specimens M_2–M_3 and mullite in specimen M_4, as proved by subsequent X-ray analysis.

Table 2 also depicts the degree of exothermic peak shifts (ΔT). These shifts exhibit the tendency of glass specimens towards bulk crystallization.

The existence of a considerable shift upon the variation of DTA sample particle sizes in the range <65 μm to 0.5–0.6 mm is a clear indication of the absence of an effective bulk nucleation mechanism.

It can be observed that in TiO_2-nucleated specimen (C) a relatively small value of ΔT (the smallest among all the specimens investigated herein) was achieved. This verifies the known marked effectiveness of TiO_2 in inducing bulk crystallization in cordierite glass ceramics. But it should be noted that the crystallization temperature of the latter specimen is relatively high and the amount of the nucleant used is quite large. These could bring about higher growth rates and alteration of original

Table 1
Chemical composition of glass specimens (wt.%)

Oxide	Specimen					
	SiO_2	Al_2O_3	MgO	TiO_2	BaO	V_2O_5
C	46.2	31.4	12.4	10	–	–
V_1	49.76	33.85	13.39	–	–	3
V_2	49.02	33.35	13.19	–	1.5	2.96
V_3	47.27	32.15	12.72	–	5	2.85
V_4	44.79	30.47	12.05	–	10	2.7
M_1	49.02	35.35	11.19	–	1.5	2.96
M_2	49.02	37.35	9.19	–	1.5	2.96
M_3	49.02	38.35	8.19	–	1.5	2.96
M_4	49.02	39.35	7.19	–	1.5	2.96

Table 2
Summary of DTA results

Specimen	First exo-peak temperature[a] (°C)	Second exo-peak temperature[a] (°C)	Peak shift for DTA exotherms (ΔT)
C	980	1166	5
V_1	–	1009 ± 5	39
V_2	–	1020 ± 6	14
V_3	–	1022 ± 3	15
V_4	–	1078 ± 7	26
M_1	–	1045 ± 5	–
M_2	–	1043 ± 3	–
M_3	–	1056 ± 4	31
M_4	–	978 ± 6	–

[a] As determined for coarse (0.5–0.6 mn) particle size specimens.

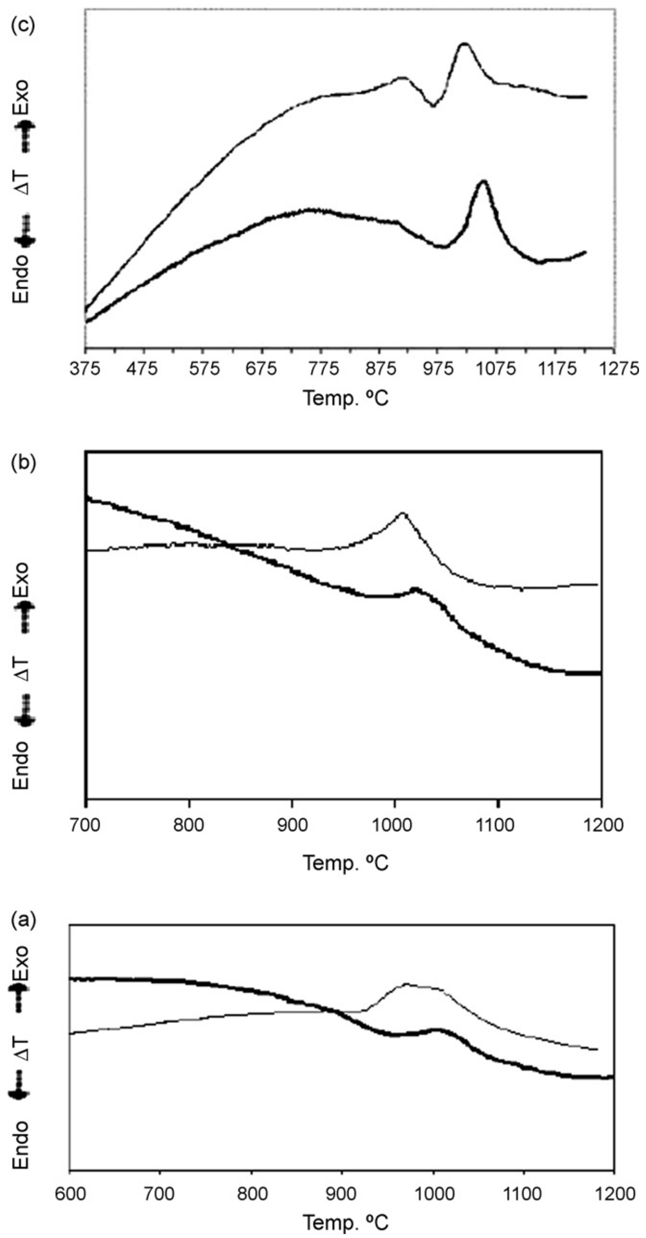

Fig. 1. DTA traces of some glass specimens. (a) V_1, (b) V_2, and (c) M_3. Specimen particle sizes: ▬, 0.5–0.6 mm; —, <65 µm.

composition, respectively, that might be detrimental to the properties. It is interesting to note that the sole specimen showing the first exothermic peak in DTA runs, which is usually attributed to the crystallization of β-quartz$_{ss}$, is specimen C.

Also it can be inferred that while the addition of little amounts of BaO (1.5 wt.%) greatly reduced the ΔT value, further addition of this oxide first had almost no effect and then raised it (10 wt.%). This is a clear implication of the fact that while the addition of little amounts of BaO promotes the bulk crystallization process, the excessive addition of this oxide has a deleterious effect on the latter process.

Shown on Table 2 is also the maximum temperature of exothermic peaks. It is apparent that while the addition of up to 5 wt.% BaO had relatively little effect on exothermic peak temperature (in comparison with the composition V_1), further additions greatly raised it (specimen V_4). This elevation of exothermic peak temperature, generally indicating less effective bulk nucleation ability can be explained by the role played by V_2O_5 in these glass structures, as follows.

When V_2O_5 assumes a network forming role in silicate glasses, the positive charge of V^{5+} as compared with neighbouring Si^{4+} ions may induce an instability in the glass structure. In this condition, V^{+5} which is a cation of relatively high ionic field strength value ($z/a^2 = 1.40$) exhibits a marked tendency for separation and greatly promotes the occurrence of microphase separation in glass.[21] Therefore, it can be suggested that in V_2O_5-containing cordierite glasses, in the same way as TiO_2 containing glasses,[1–8] after the occurrence of a metastable glass-in glass phase separation and formation of V_2O_5-rich droplets, a vanadate phase is formed within the droplets (which also were enriched in MgO and Al_2O_3) catalyzing the crystallization of α-cordierite. In fact a faint trace of a $Mg_2V_2O_7$ phase was detected in some XRD patterns of vanadium containing specimens after crystallization confirming the above deductions.

In TiO_2 containing cordierite glasses, first a metastable β-quartz solid solution is formed which at higher temperatures usually transforms to the stable α-cordierite. One of the interesting points in this work is the absence of β-quartz$_{ss}$ in the V_2O_5-containing specimens and apparently direct crystallization of α-cordierite at relatively lower temperatures, as proved by subsequent XRD analysis.

On the other hand the detrimental effect of excessive additions of BaO (e.g. 10 wt.%) on the cordierite crystallization process, may probably be attributed to its role in suppressing the phase separation process. Such suppressive effect upon phase separation also has been reported for CeO_2.[4]

Table 3 summarizes the temperatures of first endothermic effect of DTA traces, which were taken to be equal to the dilatometric softening temperatures of glass specimens.[22]

It can be seen that the addition of a relatively little amount of 1.5 wt.% BaO to these glass compositions resulted in an abrupt viscosity drop in specimen V_2, following with a small increase in viscosity upon 5 wt.% addition in specimen V_3. Finally the addition of 10 wt.% BaO resulted in higher viscosities in specimen V_4 in comparison with specimen V_1 which lacked the latter oxide. This behaviour can probably be explained by the presence of higher concentration of BaO in the continuous matrix of the phase-separated glass, controlling the overall viscosity in specimen V_2. Whereas in the specimen V_4 the elimination of phase separation which brought about a relatively uniform distribution of all constituents in the glass structure, could be the possible

Table 3
Dilatometric softening temperature of glass specimens

Specimen	Softening temperature (°C)
V_1	835 ± 3
V_2	826 ± 2
V_3	830 ± 3
V_4	838 ± 3
M_4	850 ± 3

Table 4
Crystallization products and quantities

Specimen	Major crystalline phase at first exo-peak	Major crystalline phase at second exo-peak	Final crystallinity (wt.%)
C	β-quartz$_{ss}$	Cordierite	62 ± 3
V_1	–	Cordierite	59 ± 4
V_2	–	Cordierite	92.7 ± 2.9
V_4	–	Cordierite	43.3 ± 3.1
M_3	–	Cordierite + mullite	73.5 ± 5

cause of the viscosity rise. It is proposed that the viscosity drop, brought about by the addition of 1.5 wt.% BaO, is the main cause of the enhanced tendency of the glass specimen both for surface and bulk crystallization.

In the case of specimens M_1–M_3 it can be seen that the addition of Al_2O_3 has generally resulted in the elevation of exothermic peak temperatures. One of the possible causes of this behaviour is the increase of glass viscosities due to the replacement of MgO (which is a flux) by Al_2O_3 which is an intermediate oxide well known for its role in increasing glass viscosities. The higher value of the softening temperature shown in Table 3 for glass specimen M_4 is an evidence for this effect. Obviously other factors e.g., the variation of thermodynamic driving force and glass surface tension may also be involved. In the specimen M_4 a marked drop in crystallization temperature was observed, which can be attributed to the change in the crystallization products from cordierite–mullite to a sole mullite phase as proved by XRD experiments (Table 4). In this case the entering of the glass composition into the primary phase field of mullite in the SiO_2–Al_2O_3–MgO phase diagram, radically altered all the thermodynamic factors as well as the crystallization sequences and mechanisms occurring in the glass specimen.

3.2. XRD analyses

X-ray diffractometry performed on various specimens, heat treated at their respective DTA exothermic temperatures, revealed that the TiO_2-nucleated specimens first developed a β-quartz$_{ss}$ transient phase, which transformed to cordierite at higher temperatures, in consistence to the finding of other investigators,[2–9] whereas in the V_2O_5-containing specimens cordierite was directly crystallized from the glass phase. In specimen M_1 cordierite was the sole detectable phase but in specimens M_2 and M_3 mullite also was formed along with cordierite. In specimen M_4, containing the highest amount of Al_2O_3, only mullite was detected.

The crystallized volume fractions (V) of some glass ceramic specimens were also determined using Ohlberg and Strickler[23] method, modified by Kim et al.[24] from Eq. (1) below:

$$V_{(t)} = \frac{100(I_g - I_x)}{I_g - I_b} \qquad (1)$$

where I_g, I_x and I_b are the X-ray intensity scattered by parent glass, partially crystallized glass and a mechanical mixture of oxide powders having the same composition as the parent glass, respectively. All intensities were determined at a single 2θ value.

This method is based on the principle that as the crystalline phase is formed at the expense of glass, the scattering intensity of the glass phase is proportionately reduced. In order to correct the background diffuse scattering, a mixture of crystalline compounds chemically equivalent to the parent glass is also used.

Kim et al.[24] recommended the application of the above method provided that a number of 2θ values are used instead of just a single value. Meanwhile it should be mentioned that the 2θ values should be chosen at the values where the amorphous scattering intensity of the parent glass is relatively high but is not overlapped by any crystalline diffraction peaks.

The average crystallinity contents of glass ceramic specimens based on three determinations at 2θ values of 53 (56 for specimen M_4), 45 and 15° for some specimens along with the crystallization products formed at exothermic peak temperatures are summarized in Table 4. Each value recorded in this table is the mean of three measurements carried out on different specimens.

It is obvious that specimen V_2 exhibited the highest crystallization values among all specimens.

It means that the role played by V_2O_5 as an effective nucleating agent was only gained great prominence in the presence of small amounts of BaO additive.

The above-mentioned phase separation tendency, in conjunction with the great ability of V_2O_5 in lowering surface tension of silicate glasses[25] probably may explain the great ability of this oxide in promoting the cordierite crystallization by increasing its nucleation rate. In this condition, relatively little amounts of BaO played an important role in reducing the viscosity and raising the mobility of the ions involved in the crystallization process.

In the case of specimens M_1–M_4 it can be deduced that by increasing the Al_2O_3 content, mullite which first was appeared in specimen M_2, was increased to a considerable amount in specimen M_3, eventually becoming the sole detectable crystalline product in specimen M_4. Fig. 2 show the XRD patterns of some specimens.

3.3. Microstructural investigation

The microstructural investigation of glass specimens after heat treatment, especially for relatively short holding times, may shed some light at the occurrence of crystallization process in these specimens. SEM microstructure shown in Fig. 3 reveals the occurrence of an extensive glass-in glass phase sep-

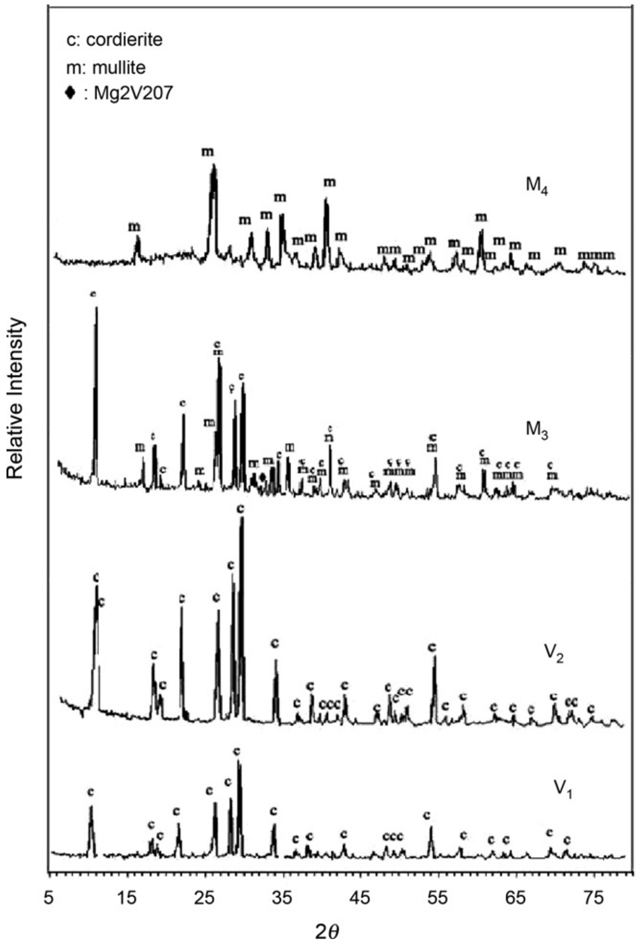

Fig. 2. XRD patterns of some glasses crystallized at their respective DTA exo-peak temperatures.

aration in the specimen V_2 after annealing at 600 °C for 1 h. The droplets 50–100 nm in diameter can be observed which are densely distributed in the glass matrix.

Fig. 4 depicts the microstructure of specimen V_2 after heat treatment at the exo-peak temperature of 1020 °C for 1 h. This micrograph has been taken from the specimen interior. It is obvious that a spherulitic growth has ocurred in this specimen.

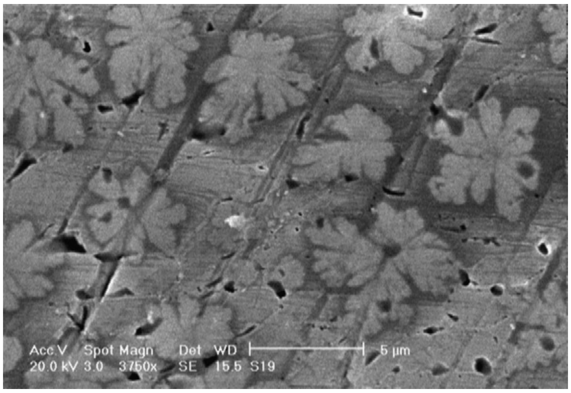

Fig. 4. SEM micrograph of specimen V_2, showing the specimen interior (polished section of fracture surface) after crystallization at 1020 °C for 1 h (bar = 5 μm).

Spherulites commonly occur in organic polymers, silicate minerals found in igneous rocks and some synthetic glasses. In these materials, which have high entropies of fusion, during crystallization at large undercoolings, nucleation of new crystals having different orientation can occur either at or in advance of the growth front. This type of nucleation which can result in spherulitic growth is favoured by low molecular mobility (i.e. high viscosity of the glass phase and by presence of impurities).[26]

All spherulites comprise fibrous crystals radiating from a common centre. In Fig. 4 the particles growing from a commen central "nucleus" are observed which have started branching in various directions. The ability of crystals to branch at a stage subsequent to nucleation is one of the important conditions for occurrence of spherulitic growth.

Fig. 5 illustrates the crystallization of the same specimen after 2 h, clearly showing the fibrous growth morphology. The secondary "arms" have started branching on the main branch of fibers at a stage of their growth. It has been shown that in contrast to the dendritic growth, crystallographic orientation is not maintained in the fibrous structure and the branching angles are not related to the crystal lattice.[26]

Fig. 6 taken from the surface of specimen V_2 shows that after a short holding time of 15 min, extensive crystallization

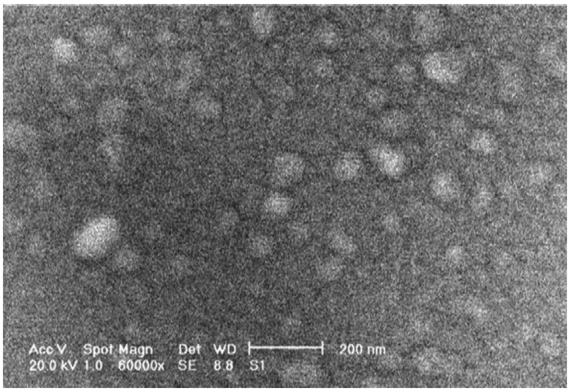

Fig. 3. SEM micrograph of specimen V_2 after annealing at 600 °C for 1 h, showing extensive glass-in glass phase separation (bar = 200 nm).

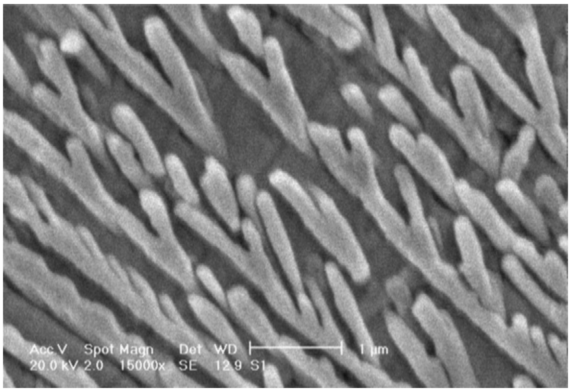

Fig. 5. SEM micrograph of specimen V_2, showing the specimen interior after crystallization at 1020 °C for 2 h (bar = 1 μm).

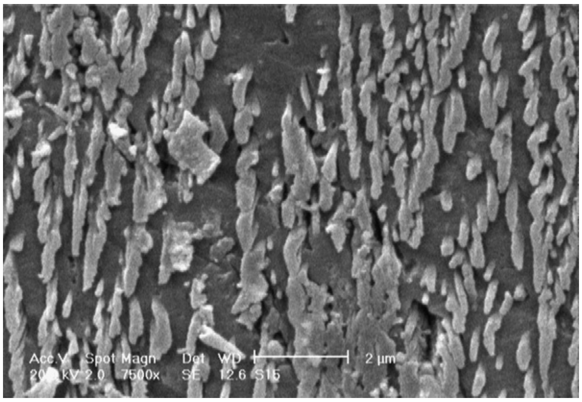

Fig. 6. SEM micrograph of specimen V_2, showing the specimen surface after crystallization at 1020 °C for 15 min (bar = 2 μm).

has occurred at the specimen surface. The crystals growing at the surface again exhibit the fibrous morphology, but there is no evidence for the occurrence of spherulitic growth. This behaviour can perhaps be explained by the very high nucleation rate at the surface of glass specimen.

Considering the fact that V_2O_5 is among the oxides having a very marked effect in reducing the glass surface tension, it is likely to have higher concentration of this oxide at the surface of glass. On the other hand vanadium may exist in the glass structure in several oxidation states. Although the V^{5+} is the most stable state but lower valencies such as V^{3+} may also be formed[25] depending on the glass composition, atmosphere and temperature. The existence of V^{5+} at the surface can apparently be promoted owing to the air contact. The lower surface tension, i.e., smaller energy barrier for occurrence of nucleation process and higher concentration of V^{+5} promoting the formation of $Mg_2V_2O_7$ nuclei, both facilitate the formation of nuclei at the surface. Considering the DTA traces shown in Fig. 1, it can be seen that the exo-peaks for specimen V_2 is much sharper in comparison with specimen V_1 especially for the fine particle size specimen. This is an evidence for the existence of higher crystallization rates in specimen V_2. It seems that BaO by lowering the glass viscosity has assisted the crystallization process both in the interior and surface of the glass specimen. The lower ΔT value for specimen V_2 as compared with specimen V_1 (Table 3) is an evidence showing the higher tendency of specimen V_2 towards bulk crystallization.

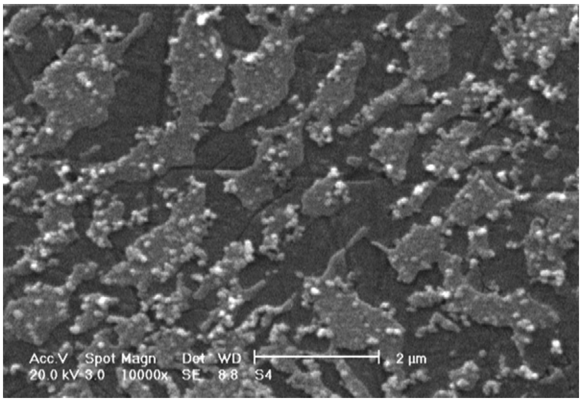

Fig. 7. SEM micrograph of specimen M_3, showing the specimen interior after crystallization at 1056 °C for 15 min (bar = 2 μm).

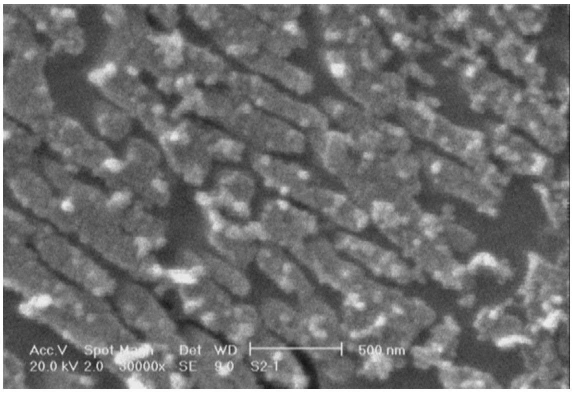

Fig. 8. SEM micrograph of specimen M_3, showing the specimen interior after crystallization at 1056 °C for 30 min (bar = 500 nm).

Figs. 7 and 8 exhibit the microstructures of specimen M_3 after 15 and 30 min heat treatment at DTA exo-peak temperature of 1056 °C, respectively. The micrographs have been taken from the specimen interior. It is interesting to note that after the relatively short holding time of 15 min at the heat treatment temperature, plate-like particles of cordierite have formed (as proved by EDX analysis) and apparently served as the heterogeneous nucleation sites for tiny mullite crystals (Fig. 7). After 30 min the cordierite plates clearly exhibited the tendency to adopt prismatic morphology (Fig. 8).

Fig. 9 exhibits the surface of specimen M_3 after 15 min heat treatment at 1056 °C. The well grown cordierite prisms and the tiny crystals of mullite formed at their surface are visible in this micrograph.

Fig. 10 shows the surface of specimen M_3 after a 30 min hold at the above temperature. The prismatic cordierite crystals are more clearly observable along with some tiny crystals of mullite nucleated and grown at their surfaces.

It can be concluded that in this specimen a tendency for faster surface crystallization of cordierite crystals existed (in comparison with the bulk crystallization), though this tendency is much less pronounced in the case of specimen M_3 as compared with specimen V_2.

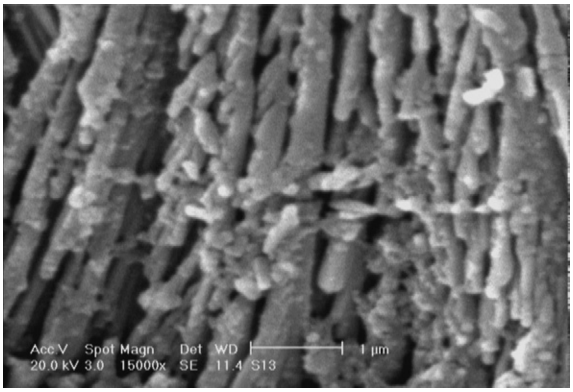

Fig. 9. SEM micrograph of specimen M_3, showing the specimen surface after crystallization at 1056 °C for15 min (bar = 1 μm).

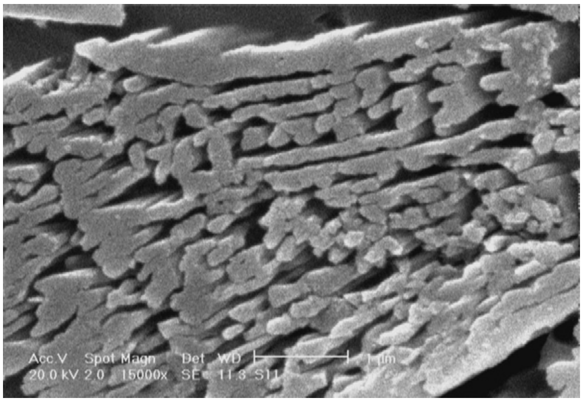

Fig. 10. SEM micrograph of specimen M_3, showing the specimen surface after crystallization at 1056 °C for 30 min (bar = 1 µm).

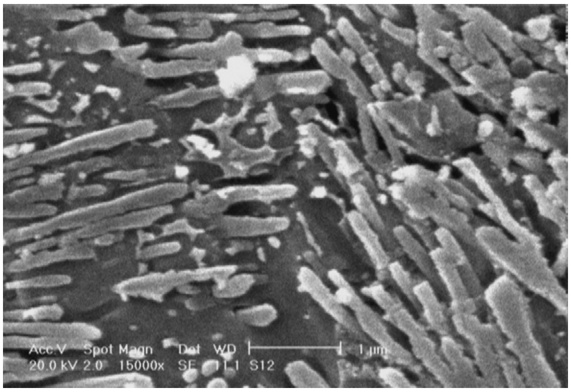

Fig. 11. SEM micrograph of specimen M_4, showing the specimen surface after crystallization at 978 °C for 1 h (bar = 1 µm).

Fig. 11 exhibits the acicular morphology of mullite crystals grown on the suface of specimen M_4 after 1 h at 978 °C. In this specimen no other crystalline phase was observed.

4. Conclusions

It can be concluded that 3 wt.% V_2O_5 in the presence of relatively little amounts of BaO can act as an effective nucleant in the crystallization of stoichiometric cordierite glass ceramics, promoting both surface and bulk crystallization of cordierite, though its effect on the surface crystallization is more pronounced.

It was shown that the crystallization proceeded via glass-in glass phase separation and formation of a vanadate phase ($Mg_2V_2O_7$) within the separated droplets serving as nuclei for the crystallization of cordierite.

Higher contents of BaO had a detrimental effect on this crystallization process by eliminating the phase separation.

Moreover, it was proved that the above additives can also be quite effective in inducing bulk crystallization in glasses with higher Al_2O_3 contents. In these glasses containing 4–5 wt.% Al_2O_3 in excess of the stoichiometric cordierite composition (added at the expense of MgO), mullite crystals can also be crystallized by nucleation and growth at the surface of previously formed cordierite crystals, eventually becoming the sole detectable crystalline phase in glasses containing 6 wt.% excess Al_2O_3.

References

1. Barry, T. I., Lay, L. A. and Morrell, R., High temperature mechanical properties of cordierite refractory glass ceramic. *Proc. Br. Ceram. Soc.*, 1975, **25**, 67–84.
2. Devekey, R. C. and Majumdar, A. J., The influence of TiO_2 on the properties of cordierite-based glass-cesamics. *Proc. Br. Ceram. Soc.*, 1975, **25**, 1–11.
3. Devekey, R. C. and Majumdar, A. J., The role of TiO_2 in the formation of cordierite glass ceramics. *Phys. Chem. Glasses*, 1975, **16**, 36–43.
4. Zdaniewski, W., Microstructure and kinetics of crystallization of $MgO–Al_2O_3–SiO_2$ glass ceramics. *J. Am. Ceam. Soc.*, 1978, **61**, 199–204.
5. Zdaniewski, W. A., Crystallization and Structure of a $MgO–Al_2O_3–SiO_2–TiO_2$ glass ceramic. *J. Mater. Sci.*, 1973, **8**, 192–202.
6. Barry, T. I., Cox, J. M. and Morrell, R., Cordierite glass ceramic effect of TiO_2 and ZrO_2 content on phase sequence during heat treatment. *J. Mater. Sci.*, 1978, **13**, 594–610.
7. Watanabe, K., Giess, E. A. and Shafer, M. W., The crystallization mecanism of high-cordierite glass. *J. Mater. Sci.*, 1985, **20**, 508–515.
8. Mc Coy, M. A. and Heuer, A. H., Microstructure characterization and fracture toughness of cordierite–ZrO_2 glass ceramics. *J. Am. Ceram. Soc.*, 1988, **71**, 673–677.
9. Vogel, W. and Holand, W., Nucleation and crystallization kinetics of an $MgO–Al_2O_3–SiO_2$ base glass with various dopants. In *Advances in Ceramics, vol. 4. Nucleation and Crystallization in Glasses*, ed. J. H. Simmons, D. R. Uhlmann and G. H. Beal. The American Ceramic Society, Columbus, Ohio, 1982, pp. 125–145.
10. Partrige, G. and Mater, Adv., Glass ceramics with controlled dielectric properties. *Adv. Mater.*, 1990, **2**, 147–150.
11. Sue, Y. J., Chen, S. Y., Lu, H. Y. and Shcn, P., Surface nucleation and cellular growth kinetics ofcordierite glass ceramics containing 3 mol% $Y_2O_3–ZrO_2$. *J. Mater. Sci.*, 1991, **26**, 1699–1704.
12. Shao, H., Liang, K. and Peng, F., Crystallization kinetics of $MgO–Al_2O_3–SiO_2$ glass ceramics. *Ceram. Int.*, 2004, **30**, 927–930.
13. Torres, F. J. and Alarcon, J., Effect of MgO/CaO ratio on the microstructure of cordierite-based glass–ceramic glazes for floor tiles. *Ceram. Int.*, 2005, **31**, 683–690.
14. Chen, G. H. and Liu, X. Y., Sintering, crystallization and properties of $MgO–Al_2O_3–SiO_2$ system glass ceramics containing ZnO. *J. Alloys Compd.*, 2007, **431**, 282–286.
15. Shao, H., Liang, K., Zhou, F., Wang, G. and Peng, F., Chacterization of cordierite-based glass ceramics produced from fly ash. *J. Non-Cryst. Sol.*, 2004, **337**, 157–160.
16. Torres, F. J., Ruiz de Sola, E. and Alarcon, J., Effect of boron oxide on the microstructure of mullite-based glass ceramic glazes for floor-tiles in the $CaO_2–MgO–Al_2O_3–SiO_2$ system. *J. Eur. Ceram. Soc.*, 2006, **26**, 2285–2292.
17. Torres, F. J., Ruiz de Sola, E. and Alarcon, J., Mechanism of crystallization of fast fired mullite-based glass ceramic glazes for floor-tiles. *J. Non-Cryst. Sol.*, 2006, **352**, 2159–2165.
18. Ferraris, M., Salvo, M. and Smeacetto, F., Cordierite–mullite coating for SiC_f/SiC composites. *J. Eur. Ceram. Soc.*, 2002, **22**, 2343–2347.
19. Devekey, R. C. and Majumdar, A. J., The influence of TiO_2 on the properties of cordierite-based glass-cesamics. *Proc. Br. Ceram. Soc.*, 1970, **37**, 772–779.
20. Mohammadi, Z. (under supervision of Marghussian, V.K.). *The effect of various nucleating agents on the crystallization behaviour of cordierite glass ceramics containing BaO and PbO. M.Sc. Thesis*. Iran University of Science and Technology, Tehran, 1994 (in Persian).
21. McMillan, P. W., *Glass Ceramic* (*2nd ed.*). Academic Press, London, 1979, p. 80.
22. Strnad, Z., *Glass Ceramic Materials, Glass Science and Technology*, *vol. 8*. Elsevier, New York, 1986, p. 146.

23. Ohlberg, S. M. and Strickler, D. W., Determination of per cent crystallinity of partly devitrified glass by X-ray diffraction. *J. Am. Ceram. Soc.*, 1962, **45**, 170–172.
24. Kim, H. S., Raawlings, R. D. and Rogers, P. S., Quantitative determination of crystalline and amorphous phases in glass ceramics by X-ray diffraction analysis. *Br. Ceram. Trans. J.*, 1989, **88**, 15–21.
25. Volf, M. B., *Chemical Approach to Glass*. Elsevier, New York, 1984, pp. 326–333.
26. McMillan, P. W., *Glass Ceramic* (*2nd ed.*). Academic Press, London, 1979, pp. 55–56.